Chemical synthesis, pharmacological characterization, and possible formation in unicellular fungi of 3-hydroxy-anandamide[1]

L. De Petrocellis,* R. Deva,[3,†] F. Mainieri,[§] M. Schaefer, T. Bisogno,[††] R. Ciccoli,[†] A. Ligresti,[††] K. Hill,** S. Nigam,[1,†] G. Appendino,[§§] and V. Di Marzo[2,††]**

Endocannabinoid Research Group, Institutes of Cybernetics* and Biomolecular Chemistry,[††] Consiglio Nazionale delle Ricerche, Pozzuoli (Napoli), Italy; Eicosanoid & Lipid Research Division & Experimental Gynecology and Breast Research,[†] Department of Gynecology & Obstetrics, Charité Medical School Benjamin Franklin, Berlin, Germany; Dipartimento di Scienze Chimiche, Alimentari, Farmaceutiche e Farmacologiche,[§] Università del Piemonte Orientale, Novara, Italy; Molekulare Pharmakologie und Zellbiologie,** Neurowissenschaftliches Forschungszentrum, Charité-Universitätsmedizin Berlin, Germany; and Ente per le Nuove Tecnologie, l'Energia e l'Ambiente Centro Ricerche Casaccia,[§§] Rome, Italy

Abstract The fungal pathogen *Candida albicans* transforms arachidonic acid (AA) into 3-hydroxyarachidonic acid [3(*R*)-HETE], and we investigated if its nonpathogenic and 3(*R*)-HETE-producing close relative, *Dipodascopsis uninucleata*, could similarly transform the endocannabinoid/endovanilloid anandamide into 3-hydroxyanandamide (3-HAEA). We found that *D. uninucleata* converts anandamide into 3-HAEA, and we therefore developed an enantiodivergent synthesis for this compound to study its pharmacological activity. Both enantiomers of 3-HAEA were as active as anandamide at elevating intracellular Ca^{2+} via TRPV1 receptors overexpressed in HEK-293 cells, while a ~70–90-fold and ~45–60-fold lower affinity at cannabinoid CB_1 and CB_2 receptors was instead observed. Patch clamp recordings showed that 3(*R*)-HAEA activates a TRPV1-like current in TRPV1-expressing HEK-293 cells. Thus, 3(*R*)-HETE-producing yeasts might convert anandamide released by host cells at the site of infection into 3(*R*)-HAEA, and this event might contribute to the inflammatory and algogenous responses associated to fungal diseases.—De Petrocellis, L., R. Deva, F. Mainieri, M. Schaefer, T. Bisogno, R. Ciccoli, A. Ligresti, K. Hill, S. Nigam, G. Appendino, and V. Di Marzo. **Chemical synthesis, pharmacological characterization, and possible formation in unicellular fungi of 3-hydroxy-anandamide. *J. Lipid Res.* 2009.** 50: **658–666.**

Supplementary key words cannabinoid • vanilloid • TRPV1 • CB1 • CB2 • endocannabinoid • endovanilloid • yeasts • inflammation • pain

Fungi belonging to the *Candida* species (Ascomycetes; class Saccharomycetes) are among the most abundant fungal pathogens and cause of infections (candidiasis) in humans. They colonize a wide range of micro environments in the human body, and not only cause damage of the skin, nails, oral, or vaginal epithelium, but are also frequently involved in life-threatening infections. *Candida* species are opportunistic pathogens and cause nosocomial infections (disseminated candidiasis) that are particularly severe in cancer patients under chemotherapy or in immunocompromised individuals (1–6). They also cause mucocutaneous infections, such as vulvovaginal candidiasis, the most prevalent superficial fungal infection in women with acquired immunodeficiency syndrome (AIDS) and diabetes mellitus, or assuming oral contraceptives, antibiotics, and corticosteroids. The symptoms of vaginal candidiasis include itching, burning, soreness, abnormal vaginal discharge, dysparunia, as well as vaginal and vulvar erythema (7). *C. albicans* is the most prevalent pathogenic fungal species, and accounts for approximately 75% of all infections in women during the child-bearing period (8). Although *C. albicans* exists in the vagina of most of the women as an innocuous commensal organism with no apparent symptoms or clinical signs (9), it can also cause untreatable problems. Thus, due to its incomplete clearance by therapy with antimycotics, several women diagnosed with an episode of sporadic vulvovaginal infection experience subsequent recurrent episodes of acute vulvovaginitis.

When looking at the major symptoms of candidiasis, particularly vulvar itching, burning, soreness, and erythema, it is possible to hypothesize that at least some of them

Manuscript received 27 June 2008 and in revised form 22 October 2008.

Published, JLR Papers in Press, November 17, 2008.
DOI 10.1194/jlr.M800337-JLR200

[1] This work is dedicated to the memory of Prof. Santosh Nigam, deceased on October 2, 2007, and of Prof. Michael J. Walker, deceased on January 5, 2008.

[2] To whom correspondence should be addressed.
e-mail: vdimarzo@icmib.na.cnr.it.

[3] Present address of R. Deva: Dermatologie, HTCC-Haut Tumor Centrum Charité, Berlin.

are: *1*) mediated by activation of transient receptor potential of vanilloid type-1 (TRPV1) channels (10, 11); and *2*) accompanied by the formation of endogenous ligands (endocannabinoids) of cannabinoid receptors of type 1 and 2 (CB_1 and CB_2), the activation of which is known to counteract itch, pain, and inflammation (12, 13). In fact, it has been shown that vulvodynia, a condition characterized by painful burning sensation, allodynia, and hyperalgesia in the region of the vulval vestibules, is accompanied by increased expression of TRPV1 receptors (14). On the other hand, inflammatory conditions causing pain are known to be counteracted by compounds that elevate the tissue levels of anandamide by inhibiting its cellular uptake or, alternatively, by interfering with its enzymatic hydrolysis (15, 16). Remarkably, there is also growing awareness that anandamide can activate TRPV1 receptors, especially during various inflammatory and pronociceptive conditions, and when its activity at CB_1 receptors is blocked and the sensitivity of TRPV1 receptors is enhanced by its phosphorylation or overexpression (17, 18).

The oxylipin 3(*R*)-hydroxy-5,8,11,14-eicosatetraenoic acid [3(*R*)-HETE] (**Fig. 1**), an intermediate of the β-oxidation of arachidonic acid (AA), has an important biological role in the life cycle of fungi, and was first described in the nonpathogenic species *Diposascopsis uninucleata* (19), where its formation is associated with morphogenesis during the sexual life cycle. During infection by *C. albicans*, host cells produce AA to counteract this process, but *Candida* is able to utilize AA released from host cells to form 3(*R*)-HETE and related compounds through a well-characterized process utilizing its fatty acid β-oxidation pathway (20). 3(*R*)-HETE is associated with hyphal forms of *Candida* and is important for their anchorage to host cells during infection (21). Thus, *Candida* can chemically modify the metabolites of the host cell to facilitate infection. Notwithstanding the presence of a C-3 hydroxyl, 3(*R*)-HETE is a substrate of cyclooxygenase-2 (an enzyme up-regulated during candidiasis), thereby generating compounds that, like 3(*R*)-hydroxy-PGE_2, are capable to induce interleukin-6 gene expression via the EP_3 receptor (22, 23), and to ultimately trigger further inflammation cascades.

In view of the chemical similarity between anandamide and AA, and their capability to be both recognized by several oxygenating enzymes (see for review Ref. 24), we have hypothesized that a 3(*R*)-HETE-producing fungus would be capable to convert anandamide into its 3-hydroxy-derivative, thus potentially altering its cannabinoid and vanilloid profile at the site of infection. To investigate this issue and evaluate its clinical implications, we have studied the metabolism of anandamide by *D. uninucleata* (19) and have developed an enantiodivergent synthesis of 3-hydroxy-anandamide (3-HAEA) (Fig. 1), a so-far unknown oxylipin, to explore its biological activity.

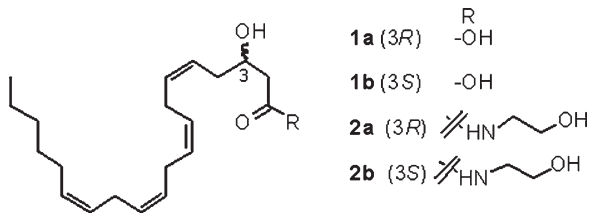

Fig. 1. Chemical structures of 3-HETE and 3-hydroxy-anandamide (3-HAEA) isomers.

MATERIALS AND METHODS

Fungal culture and incubation with AA

D. uninucleata (Lipomycetaceae, Saccharomycetales, Saccharomycetidae, Saccharomycetes, Ascomycota, UOFS-Y128, South African Strain obtained from Prof. Kock., The University of the Orange Free State, Bloemfontein, South Africa) was grown in yeast nitrogen base medium up to the initial phase of the sexual cycle. Two aliquots of 50 ml of culture were incubated with 100 μM anandamide. Fifty ml of culture were incubated with 100 μM AA as a positive control. A fourth 50 ml aliquot was incubated with vehicle (10 μl methanol) as a negative control. After 6 h of incubation at 37°C the first 50 ml batch of anandamide incubate and the batches incubated with AA and vehicle were spun down at 300 *g*. The pellet (2.5 ml) was suspended in 4 ml of phosphate buffered saline and subjected to mechanical breaking under liquid N_2. After 12 h of incubation, the second batch of anandamide incubate was subjected to mechanical breaking. Broken cells were subjected to lipid extraction with 4 ml of methanol and 8 ml of chloroform. After separation of the organic phase, the residual phase was extracted two more times with 8 ml of chloroform. Chloroform phases were pooled and dried under vacuo. The extract was dissolved in 1 ml of methanol. One hundred microliters of this solution were analyzed by HPLC carried out on a reverse phase column (25 cm × 4.6 mm id × 5 μm) eluted with methanol/water/acetic acid 85/15/0.01. Major peaks were analyzed by LC-ESI-IT-TOF and APCI-TOF.

Synthesis of 3(*R*)-HAEA and 3-HAEA, 3-hydroxy-anandamide (3(*S*)-HAEA) (synthesis of 3(*R*)-HAEA as an example).

General synthetic procedures. Gravity column chromatography (GCC): Merck Silica Gel (70–230 mesh). HPLC: Waters 1523 binary HPLC instrument with dual lambda detector 2487. NMR: Jeol Eclipse (300 MHz and 75 MHz for ^1H and ^{13}C, respectively). Chemical shifts are reported in δ values downfield from TMS. CH_2Cl_2 and THF were dried by filtration over alumina directly in the reaction flask. Petroleum ether refers to the fraction boiling between 40°C and 60°C. All reactions were conducted under nitrogen in dry solvents unless stated otherwise. Monitoring by TLC was done on Merck 60 F_{254} (0.25 mm) plates, that were visualized by UV inspection and/or staining with 5% H_2SO_4 in ethanol and heating. Organic phases were dried with Na_2SO_4 before evaporation.

(R,S) - *Benzhydryl but-2-enoate epoxide (4a,b).* To a cooled (ice bath) solution of benzhydryl but-2-enoate (2.0 g, 7.9 mmol) in dichloromethane (100 ml), solid $NaHCO_3$ (333 mg, 3.95 mmol, 0.5 equiv.) was added, and to this suspension a solution of 85% *meta*-chloroperoxybenzoic acid (MCPBA, 1.31 g, 9.5 mmol, 1.2 equiv.) in dichloromethane (50 ml) was added dropwise over 15 min. After stirring 1 h at 0°C and 10 h at room temperature, the reaction was worked up by filtration over neutral alumina to remove *meta*-chlorobenzoic acid and unreacted MCPBA, and the filtration cake was washed with CH_2Cl_2. The pooled filtrates were evaporated, and the residue was purified by GCC on silica gel (75 g, petroleum ether-EtOAc 8:2 as eluant), affording 1.47 g (69%) **4a,b** as a colorless oil. ^1H NMR (300 MHz, $CDCl_3$): δ 7.37–7.30 (10H, m, Ar-H), 6.96 (1H, s, $Ar_2\underline{C}HO$), 3.33 (1H, m,

H-3), 2.84 (1H, t, J = 4.8 Hz, H-2a), 2.69 (2H, m, H-2b + H-4a), 2.57 (1H, dd, J =4.8, 2.7 Hz, H-4b); ^{13}C NMR (50 MHz, $CDCl_3$): δ 169.7 (s), 140.3 (s), 128.9 (d), 128.3 (d), 127.4 (d), 77.7 (d), 48.2 (d), 46.8 (t), 38.6 (t); CIMS 269 $(M+H)^+$ $(C_{17}H_{16}O_3 + H)^+$.

(S) - *Benzhydryl but-2-enoate epoxide (4a).* To a stirred solution of **4a,b** (2.0 g, 7.45 mmol) in THF (0.2 ml), (*S,S*)-salen-Co. (10 mg, activated by reaction with acetic acid in toluene) was added. After complete solubilization, water (72 μl) was added, and stirring was continued at room temperature by monitoring the course of the reaction by HPLC (methanol-water gradient, from 5:5 to 9:1 in 20 min). After 120 h, the reaction was worked up by the addition of 2N H_2SO_4 and extraction with EtOAc. After washing with brine and drying, the organic phase was evaporated, and the residue was purified by GCC on silica gel (25 g, petroleum ether/ether 8:2 as eluant) to afford 700 mg (35%) of **4a** as a colorless oil. The optical purity, checked after conversion to **5a** and HPLC analysis of its diastereomeric Mosher esters, was >95%. Conditions of analysis: Simmetry C-18 column, methanol/water 7:3 as eluant, Rt of *R*-ester: 11.60 min; Rt of *S*-ester: 14.00 min.

(R)-*Benzhydryl 3-hydroxyhex-5-ynoate (5a).* To a cooled (−25°C) solution of trimethylsilyl acetylene (2.2 ml, 1.5 g, 14.9 mmol, 2 equiv.) in dry toluene (15 ml), butyl lithium (2.5 M in hexanes, 6.0 ml, 14.9 mmol. 2 equiv) was added dropwise. The resulting milky suspension was stirred at −15°C for 15 min, and then warmed to 0°C by replacement of the dry ice/acetone with a ice/water cooling bath. Transmetalation was carried out by the dropwise addition of diethylaluminum chloride (1.0 M in hexanes, 15.0 ml, 149 mmol, 2 mol. equiv.) and stirring at 0°C for 1 h, and then a solution of the (*S*)-epoxide **4a** (2.0 g, 7.45 mmol) in toluene (10 ml) was added dropwise. After stirring for 2 h at room temperature, the solution was worked up by neutralization with sat. NH_4Cl, acidification with 1 M HCl, and extraction with EtOAc. The organic phase was dried and evaporated, and the residue was dissolved in THF (10 ml) and then treated at 0°C with 1.0 M TBAF (7.45 ml, 7.45 mmol) in THF. After stirring 30 min at 0°C, the reaction was worked up by the addition of brine, and extracted with ether. The organic phase was dried (Na_2SO_4) and evaporated, and the residue was purified by GCC on silica gel (25 g) with petroleum ether-ether 7:3 as eluant, affording 1.3 g (61%) **5a** as a colorless oil. ^{1}H NMR (300 MHz, $CDCl_3$): δ 7.37–7.30 (10H, s, Ar-H), 6.92 (1H, s, Ar_2CHO), 4.22 (1H, s, H-3), 3.04 (1H, d, J = 4.2 Hz, H-6), 2.80 (1H, dd, J = 16.8, 3.9 Hz, H-2a), 2.70 (1H, dd, J = 16.8, 8.4 Hz, H-2b), 2.44 (1H, m, H-4a), 2.05 (1H, m, H-4b); ^{13}C NMR (50 MHz, $CDCl_3$): δ 172.1 (s), 140.4 (s), 128.9 (d), 128.3 (d), 127.4 (d), 77.7 (d), 48.2 (d), 46.8 (t), 38.6 (t); CIMS: 295 $(M+H)^+$ $(C_{19}H_{18}O_3 + H)^+$.

Benzhydryl 3-hydroxyicosa-5,8,11,14-tetraynoate (7a). To a solution of **5a** (1.0 g, 3.4 mmol, 1 equiv) and 1-bromotetradeca-2,5,8-triyne (**6**, 906 mg, 3.4 mmol, 1 equiv) in DMF (5ml), a well-amalgamated (mortar) mixture of CuI (1.3 g, 6.8 mmol, 2 equiv), NaI (1.0 g, 6.8 mmol, 2 equiv), and K_2CO_3 (705 mg, 5.1 mmol, 1.5 equiv) was added. The suspension was stirred at room temperature under nitrogen atmosphere for 10 h, and then worked up by the addition of 30% ammonia and ether. The organic phase was washed with brine, dried, and evaporated, and the residue was purified by GCC on silica gel (25 g, petroleum ether-ether 4/6 as eluant) to afford 1.1 g (78%) **7a** as an orange oil. ^{1}H NMR (300 MHz, $CDCl_3$): δ 7.33–7.25 (10H, s, Ar-H), 6.91 (1H, s, Ar_2CHO), 4.17 (1H, s, H-3), 3.12 (6H, br s, H-7a,b + H-10a,b + H-13a,b), 2.77 (1H, dd, J = 16.8, 3.9 Hz, H-2a), 2.63 (1H, dd, J = 16.8, 8.4 Hz, H-2b), 2.40 (2H, m, H-16a,b), 2.10 (2H, m, H-17a,b), 1.45 (2H, m, H-18a,b), 2.10 (2H, m, H-19a,b), 0.89 (3H, t, J = 6.5 Hz, H-20); ^{13}C NMR (50 MHz, $CDCl_3$): δ 171.6 (s), 140.0 (s), 128.7 (d), 128.2 (d), 127.2 (d), 81.6 (s), 78.2 (d), 76.8 (s), 76.0 (s), 75.2 (s), 74.7 (s), 74.3 (s), 66.8 (d), 40.7 (t), 31.3 (t), 28.6 (t), 28.5 (t), 26.8 (t), 22.4 (t), 18.9 (t), 14.2 (t), 10.0 (t); CIMS: 479 $(M+H)^+$ $(C_3H_{34}O_3 + H)^+$.

*(3*R*, 5Z,8Z,11Z,14Z)-3-Hydroxyicosa-5,8,11,14-tetraenoic acid [3*(R)*-HETE, 1a].* To a suspension of $Ni(OAc)_2$ (831 mg, 4.7 mmol) in absolute ethanol (10 ml), $NaBH_4$ (178 mg, 4.7 mmol) was added. After stirring at room temperature for 10 min, ethylendiamine (334 mg, 4.7 mmol) was added dropwise, and hydrogen was then bubbled through the suspension for 10 min. A solution of **7a** (1.0 g, 2.1 mmol) in abs. ethanol (5 ml) was next added dropwise, and the reaction was stirred at room temperature, monitoring its course by TLC on silver-coated plates (petroleum ether-ether 4:6; Rf starting material: 0.50; Rf reaction product: 0.70). After 250 min, the reaction was worked up by filtration over Celite, dilution with water, and extraction with ether. The organic phase was washed with 2N H_2SO_4, dried (Na_2SO_4), and evaporated, and the residue was dissolved in CH_2Cl_2 (6.5 ml) and treated with trifluoroacetic acid (TFA, 100 μl). After stirring at room temperature for 10 min, the reaction was worked up by dilution with brine and extraction with CH_2Cl_2. The organic phase was washed with brine, dried, and evaporated, and the residue was purified by GCC on silica gel (12.5 g, petroleum ether/ether 3:7 as eluant) to afford 342 mg (51% from **7a**) **1a** as a yellowish oil, whose ^{1}H NMR and ^{13}C NMR data were identical to those reported in the literature (29).

*(3*R*, 5Z,8Z,11Z,14Z)-3-Hydroxyicosa-5,8,11,14-tetraenoic acid ethanolamide [3*(R)*-HEAA, 2a].* To a solution of **1a** (50 mg, 0.14 mmol) in CH_2Cl_2 (1ml), triethylamine (78 μl) and PPAA (50% in EtOAc, 102 μl) were added. After stirring 30 min at room temperature, ethanolamine (78 μl, 57 mg, 0.56 mmol, 4 equivalents) was added, and reaction was stirred at room temperature for 2 h, and then worked up by the addition of 2N H_2SO_4 and dilution with CH_2Cl_2. The organic phase was washed with brine, dried, and evaporated, and the residue was purified by GCC on silica gel (2.5 g, petroleum ether/EtOAc 7:3 as eluant), to afford 23 mg (43%) **2a** as a pale-yellow oil. ^{1}H NMR (300 MHz, $CDCl_3$): δ 6.28 (1H, br s, NH), 5.36 (2H, br m, H-6 + H-14), 5.35 (6H, br m, H-5 + H-8 + H-9 + H-11 + H-12 + H-15), 4.00 (1H, br m, H-3), 3.71 (2H, br t, J = 5.8 Hz, H-2'), 3.45 (2H, br m, H-1'), 2.81 (6H, br m, H-7a, b + H-10a,b + H-13a,b), 2.41 (1H, dd, J = 16.8, 4.0 Hz, H-2a), 2.29 (1H, dd, J = 16.8, 8.4 Hz, H-2b), 2.25 (2H, br m, H-4a,b), 2.01 (2H, br m, H-16a,b), 1.40-1.20 (6H, br m, H-17a,b + H-18a,b + H-19a, b), 0.89 (3H, br t, J = 6.2 Hz, H-20); CIMS: 346 $(M+H-H_2O)^+$ $(C_{22}H_{37}NO_3 + H - H_2O)^+$.

Mass spectrometric analysis of synthetic and natural 3-HAEA

Liquid chromatography-atmospheric pressure chemical ionization-mass spectrometry (LC-APCI-MS) was performed by using a Shimadzu high-performance liquid chromatography (HPLC) apparatus (LC-10ADVP) coupled to a Shimadzu quadrupole mass spectrometer (LCMS-2010) via a Shimadzu APCI interface. The temperature of the APCI source was 400°C; the HPLC column was a Phenomenex (5 μm, 150 × 4.5 mm) reverse phase column, eluted by using methanol/water/acetic acid 85/15/0.01 as the mobile phase with a flow rate of 1 ml/min. High resolution LC-MS/MS analysis was carried out with liquid chromatography-electrospray-ion trap-time of flight (LC-ESI-IT-ToF) by using an IT-ToF mass spectrometer (Shimadzu) in conjunction with an LC-20AB (Shimadzu). LC separation was performed using a Discovery® C18 column (15cm × 2.1mm, 5 μm) and methanol/water/acetic acid 85/15/0.01 as the mobile phase with a flow rate

of 0.15 ml/min. Identification of compounds was determined using electrospray ionization (ESI) in positive mode, with nebulizing gas flow: 1.5 l/min and CDL temperature of 250°C.

TRPV1 receptor assays

HEK-293 cells stably overexpressing recombinant the human TRPV1 cDNA (17) were grown as monolayers in minimum essential medium supplemented with nonessential amino acids, 10% fetal calf serum, and 2 mM glutamine, and maintained under O_2/CO_2 (95%/5%) at 37°C. The effect of test substances on intracellular Ca^{2+} concentration was determined by using Fluo-4, a selective intracellular fluorescent probe for Ca^{2+}. On the day of the experiment, the cells were loaded for 1 h at 25°C with Fluo-4 methylester (Invitrogen) 4 μM in dimethyl sulfoxide containing 0.02% Pluronic® (Invitrogen), in minimum essential medium without FBS. After the loading, cells were washed twice in Tyrode's buffer pH 7.4 (NaCl 145 mM; KCl 2.5 mM; $CaCl_2$ 1.5 mM; $MgCl_2$ 1.2 mM; D-Glucose 10 mM; HEPES 10 mM pH 7.4), resuspended in Tyrode's buffer and transferred (50–60,000 cells) to the quartz cuvette of the fluorescence detector (Perkin-Elmer LS50B) under continuous stirring. Experiments were carried out by measuring cell fluorescence at 25°C (λ_{EX} = 488 nm, λ_{EM} = 516 nm) before and after the addition of the test compounds at various concentrations (1 nM–50 μM). Agonist activity was determined in comparison to the maximum increase of intracellular Ca^{2+} due to the application of 4 μM ionomycin (Sigma). EC_{50} values were determined as the concentration of test substances required to produce half-maximal increases in $[Ca^{2+}]_i$. All determinations were at least performed in triplicate. Curve fitting and parameter estimation was performed with GraphPad Prism® (GraphPad Software Inc., San Diego, CA). Statistical analysis of the data was performed by ANOVA at each point using ANOVA followed by Bonferroni's test. Differences were considered significant at the $P < 0.05$.

Binding assays at CB_1 and CB_2 receptors

Membranes from HEK-293 cells transfected with the cDNA encoding for the human recombinant CB_1 receptor (B_{max}= 2.5 pmol/mg protein) or the human recombinant CB_2 receptor (B_{max}= 4.7 pmol/mg protein), were incubated with [^{3}H]CP-55,940 (0.14nM, K_d=0.18 nM or 0.084 nM, K_d= 0.31 nM, respectively, for the CB_1 or CB_2 receptor) as the high affinity ligand, and displaced with 1 μM WIN 55212-2 as the heterologous competitor for nonspecific binding (K_i values 9.2 nM and 2.1 nM, respectively, for the CB_1 and CB_2 receptor). All compounds were tested following the procedure described by the manufacturer (Perkin Elmer, Italy). Displacement curves were generated by incubating increasing concentrations of compounds (10 nM–5 μM) with [^{3}H]CP-55,940 for 90 min at 30°C. K_i values were calculated by applying the Cheng-Prusoff equation to the IC_{50} values (obtained by GraphPad Prsim®) for the displacement of the bound radioligand by the test compounds. Data are means ± SEM of at least n = 3 experiments.

Patch clamp electrophysiology

HEK 293 cells stably expressing TRPV1 were recorded in a continuously perfused recording chamber (500 μl volume) mounted on the stage of an inverted microscope. The standard bath solution consisted of (in mM): 140 NaCl, 5 CsCl, 2 $MgCl_2$, 10 HEPES, 10 D-glucose pH 7.4 (NaOH). The pipette solution contained (in mM) 140 CsCl, 4 $MgCl_2$, 5 EGTA, 10 HEPES, pH 7.2 (CsOH). All experiments were performed at room temperature using a HEKA EPC-9 amplifier (HEKA Electronics, Germany). Patch pipettes of 3–5 MΩ were fabricated from borosilicate glass capillaries. Experiments were carried out and analyzed under the control of the Pulse and Pulsefit software (HEKA Electronics, Germany). Series resistances were <10 MΩ, and were compensated by 75–85%. Stated membrane potentials always refer to the physiological inner side of the membrane.

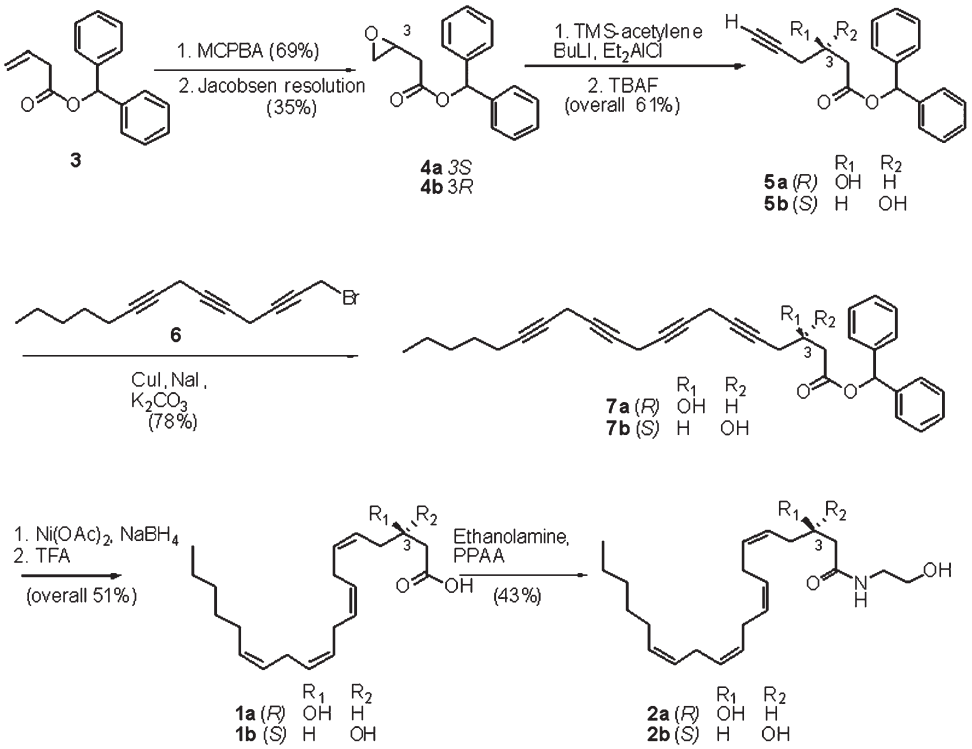

Fig. 2. Asymmetric synthesis of 3(R)- and 3(S)-HAEA (2a and 2b, respectively). Yields for 2a are given as representative.

RESULTS

Enantiodivergent synthesis of 3-hydroxy-eicosatetraenoic acid (3-HETE) and 3-HAEA enantiomers

Synthetic 3(*R*)-HETE was obtained by semisynthesis from 5,6-epoxyarachidonic acid (25), or, alternatively, by total synthesis from (*R*)-epichlorohydrin (26); we developed an alternative and more versatile asymmetric enantioselective synthesis of enantiomers 3(*R*)-HAEA (2a) and 3(*S*)-HAEA (2b) from benzhydryl-but-2-enoate oxide (3) (**Fig. 2**). Jacobsen hydrolytic kinetic resolution was used to establish the C-3 stereocenter and prepare multigram amounts of the enantiopure (>95% ee) epoxides 4a and 4b, next regioselectively opened with the acetylenic alane derived from trimethylsilylacetylene (27) to give, after desilylation, the C-6 propargylic alcohols **5a** and **5b**. Coupling with the tri-

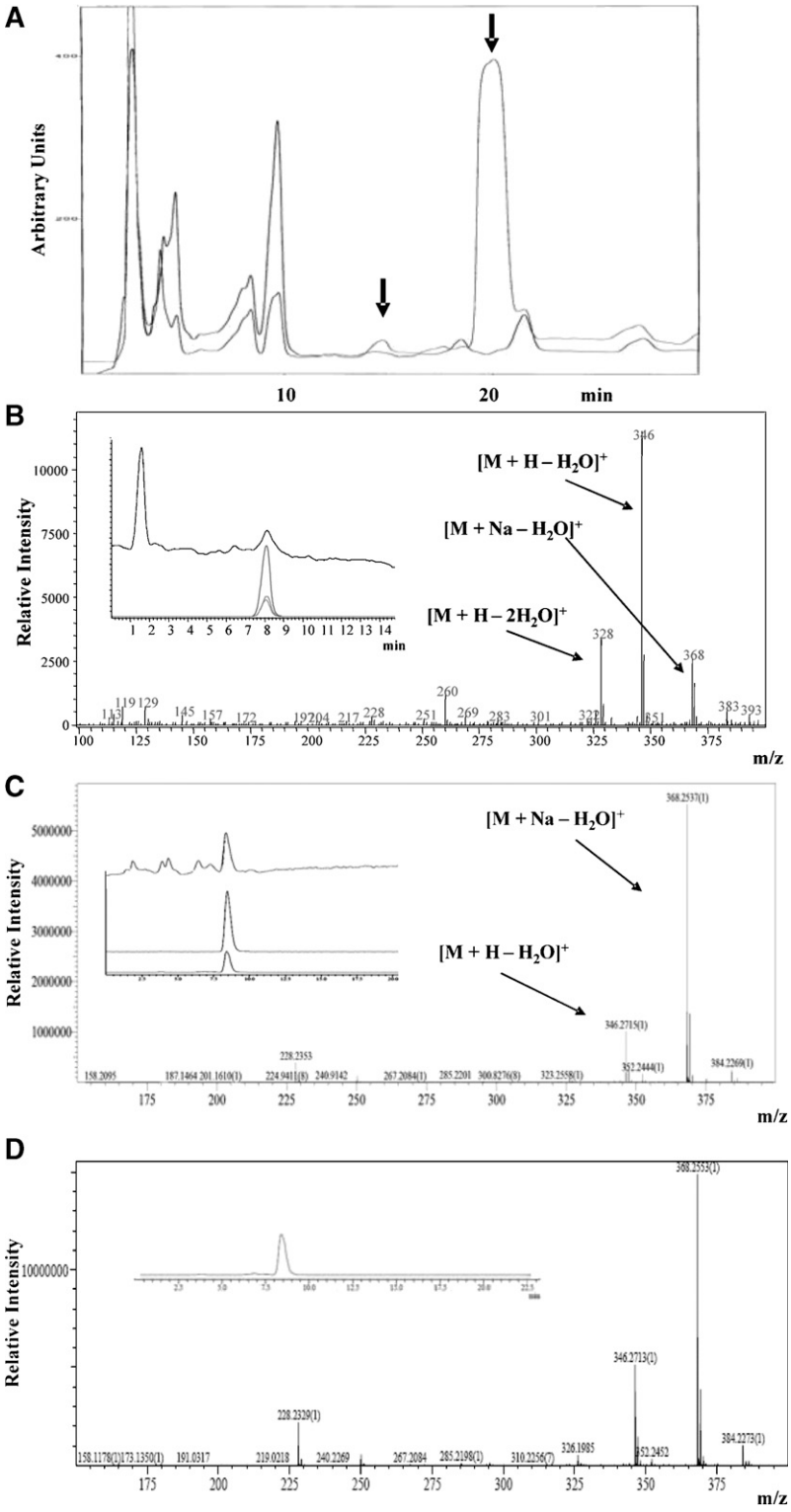

Fig. 3. Identification of 3-HAEA in *D. uninucleata* cultures incubated with anandamide. A: HPLC chromatogram of the organic extract of *D. uninucleata* culture incubated for 6 h with 100 μM anandamide (upper line) and the negative control (from extracts of cells incubated with no anandamide, lower line). The arrows indicate the retention times of anandamide (20 min) and of the new formed peak (14 min) that was subsequently analyzed by LC-MS and LC-MS-MS. B: Mass spectrum (LC-APCI-MS) of HPLC fraction 13–16 shows peaks at m/z = 368, 346, and 328 identified as $[M + Na - H_20]^+$, $[M + H - H_20]^+$ (base peak), and $[M + H - 2H_20]^+$, respectively. The inset shows total ion current spectra of prepurified *D. uninucleata* organic extract with the relative selected extracted ions. C: Mass spectrum with high mass accuracy obtained by LC/MS/IT-ToF analysis of the HPLC fraction 13–16. Peaks at m/z = 368.2537 and 346.2715 correlate with the chemical formula $[C_{22}H_{35}NO_2 + Na - H_2O]^+$ and $[C_{22}H_{35}NO_2 + H - H_2O]^+$, respectively, within ≤ 8 ppm. The inset shows the total ion current spectrum of prepurified *D. uninucleata* organic extract with the relative selected extracted ions. D: Mass spectrum with high mass accuracy obtained by LC/MS/IT-ToF analysis of a synthetic standard (1 nmol) of 3(R)-HAEA. The inset shows the total ion current spectrum of the analysis with the relative selected extracted ion. It should be noted that the observed mass spectra are also compatible with the molecular formula and fragmentation pattern of 2,3-Δ-AEA, of which, unfortunately, we do not possess an authentic standard.

acetylenic C-14 propargylic bromide **6** (28) under copper (I) promotion, afforded the C-20 tetrayne esters **7a** and **7b**. Semireduction with Nickel boride to the corresponding tetraenic esters, and deprotection with trifluoroacetic acid led to the enantiomeric HETEs **1a** and **1b**, eventually coupled with ethanolamine under PPAA (propylphosphonic acid anhydride) (29) promotion to afford 3(*R*)-HAEA and 3(*S*)-HAEA (**2a** and **2b**, respectively). After amidation with ethanolamine, both homochiral 3-HAEA enantiomers (>95% ee) were used for biological profiling.

Identification of 3-HAEA in *D. uninucleata* incubates

Lipid extracts from incubates of the *D. uninucleata* with anandamide or vehicle were purified by semipreparative reverse-phase HPLC (**Fig. 3A**). The HPLC fractions at 13–16 min contained a component more hydrophilic than anandamide (retention time 20 min, see later discussion), which was produced in an yield of approximately 5% with respect to the peak of anandamide. This HPLC component was the only peak that was virtually absent from the HPLC chromatogram relative to the incubate carried out in the absence of anandamide (Fig. 3A, red line). Under the same incubation conditions approximately 10% of AA was transformed into 3-HETE (data not shown). Preliminary identification of this peak was performed by LC-APCI-MS analysis. This allowed the identification of the LC peak at retention time 8 min. The mass spectrum exhibits the ions at $m/z = 346$, as the base peak, and 328, due to the loss of one or two water molecules from the molecular ion peak, respectively (Fig. 3B). The identity of 3-HAEA was established through use of reverse-phase HPLC coupled to electrospray IT-ToF mass spectrometry, which accomplishes high accuracy mass measurement. The mass spectrum, in positive mode, of the HPLC fraction 13–16 of Fig. 3A displays a major HPLC peak at 8 min containing a component with a base peak ion at $m/z = 368.2537$ identified as the Na^+ adduct of the molecular ion of 3-HAEA with loss of one molecule of water $[M + Na - H_20]^+$ ($C_{22}H_{35}NO_2 + Na$). This peak was more abundant than fragment $[M + H - H_20]^+$, at $m/z = 346.2715$ ($C_{22}H_{35}NO_2$) (Fig. 3C). The retention time on HPLC and the measured masses for each peak coincided with the theoretical ones calculated from the corresponding chemical formula within ≤ 8 ppm (data not shown). The peak at $m/z = 368.2537$ was subjected to further analysis by MS^2, which yielded a major fragment at $m/z = 350.2410$ (data not shown), corresponding to the chemical formula of $C_{22}H_{33}NO + Na$, and interpreted as the parent ion with loss of one further molecule of water ($[M + Na - 2H_20]^+$). The major peak in the chromatogram shown in Fig. 3A (retention time 20 min) was identified as anandamide, which also yields as the only peak the molecular ion plus Na^+ ($C_{22}H_{37}NO_2 + Na$, $m/z = 370.2750$, within 8.9 ppm of the expected mass). In agreement with the identity of the unknown component as 3-HAEA, synthetic 3(R)-HAEA was analyzed by LC-IT-ToF under the same conditions and yielded a peak at exactly the same retention time and with a superimposable MS fragmentation pattern, with m/z values almost identical (within 2 ppm) to those of the compound isolated from *D. uninucleata* extracts (Fig. 3D). It must be pointed out, however, that the observed mass spectrum is also compatible with the molecular formula and fragmentation pattern of the potential biosynthetic precursor of 3-HAEA via the β-oxidation pathway (i.e., the 2,3-Δ-AEA, of which, unfortunately, we do not possess an authentic standard). At any rate, when the synthetic compound was coanalyzed with the extract, only one homogeneous peak with this fragmentation pattern was observed (data not shown).

Activity of 3(*R*)-HAEA and 3(*S*)-HAEA at human recombinant TRPV1 receptors

Using a fluorometric test, we showed that human TRPV1-expressing HEK293 cells exhibit a sharp increase in intracellular Ca^{2+} upon application of 3(*R*)-HAEA and 3(*S*)-HAEA. The activity of the compounds was normalized to the maximum intracellular Ca^{2+} elevation generated by application of 4 μM ionomycin. Using this test, we determined the concentration for half-maximal activation to be 0.45 ± 0.02 μM (hill slope 0.92 ± 0.02) and 0.39 ± 0.02 μM (hill slope 1.02 ± 0.02), respectively (**Fig. 4** and **Table 1**). The maximal effect at 10 μM was 78.3 ± 0.6% and 79.4 ± 0.7% of the effect of ionomycin 4 μM. Iodoresiniferatoxin (0.1 μM), a known blocker of TRPV1, inhibited the effect at 10 μM of both (96.8 ± 3.2% and 96.6 ± 3.7% inhibition, respectively). 3(*R*)-HETE and 3(*S*)-HETE were significantly less active (Fig. 4).

Activity of 3(*R*)-HAEA on TRPV1-mediated currents

We performed whole-cell voltage clamp recordings to test whether TRPV1 currents can directly be activated by 3(*R*)-HAEA. HEK-293 cells heterologously expressing human TRPV1 responded with large inward and outward current to the application of 20 μM 3(*R*)-HAEA (**Fig. 5A**). The current voltage curves obtained resemble the basic characteristics of TRPV1. Moreover, the elicited current could be blocked by the TRPV1 antagonist capsazepine

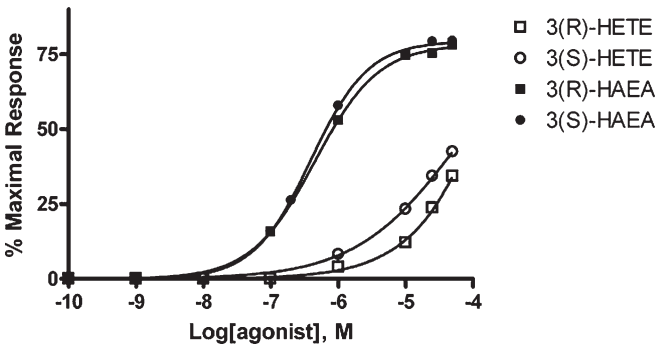

Fig. 4. Dose-response curves for the effect of the 3-hydroxy-derivatives on intracellular Ca^{2+} in HEK-293 cells overexpressing the human recombinant TRPV1 receptor. Data are expressed as percent of the effect of 4 μM ionomycin (maximal response). Data are means of at least N = 3 experiments. Standard errors are not shown for the sake of clarity and were never higher than 10% of the means. HETE, hydroxyeicosatetraenoic acid; HAEA, hydroxy-anandamide.

TABLE 1. Affinity of 3-hydroxy-derivatives at human recombinant CB_1 and CB_2 receptors and functional activity at human recombinant TRPV1 receptors

Compound	K_i at CB_1 (μM)	Max tested (% displacement)	K_i at CB_2 (μM)	Max tested (% displacement)	EC_{50} on TRPV1 (μM)	Max tested (% ionomycin)
AEA	0.02 ± 0.01	5 μM (98.1%)	0.11 ± 0.02	5 μM (97.0%)	0.28 ± 0.03	50 μM (60.4%)
3(*R*)-HAEA	1.85 ± 0.27	5 μM (66.16%)	6.43 ± 0.77	10 μM (68.8%)	0.45 ± 0.04	50 μM (78.3%)
3(*S*)-HAEA	1.46 ± 0.33	5 μM (72.09%)	4.85 ± 0.38	10 μM (84.1%)	0.39 ± 0.03	50 μM (79.4%)
3(*R*)-HETE	>5	5 μM (35.51%)	>5	10 μM (23.8%)	>50	50 μM (34.3%)
3(*S*)-HETE	>5	5 μM (46.56%)	>5	10 μM (32.4%)	>50	50 μM (42.4%)

HETE, hydroxyeicosatetraenoic acid; HAEA, hydroxy-anandamide. The affinity of the 3-hydroxy-derivatives is expressed in terms of absolute K_i (μM) for the displacement of [^{3}H]CP-55,940 from human recombinant CB_1 and CB_2 receptors. K_i values are calculated by applying the Cheng-Prusoff equation to the IC_{50} values for the displacement of the bound radioligand by increasing concentrations of the test compound. The maximal concentrations tested and their effects are also shown. The functional activity at TRPV1 receptors was measured by assessing the effects of the drugs on TRPV1-mediated elevation of intracellular Ca^{2+} concentrations, and the potency in this assays is reported as IC_{50} values. Efficacy is reported as the effect of the maximal concentration tested as % of the maximum observable effect on intracellular Ca^{2+} concentrations (i.e., that of 4 μM ionomycin, assessed in each experiment). Data are means ± SEM of at least n = 3 experiments.

(Fig. 5B). No current was evoked in control HEK293 cells by 3(R)-HAEA (data not shown).

Affinity of 3(*R*)-HAEA and 3(*S*)-HAEA at human recombinant CB_1 and CB_2 receptors

Both enantiomers of 3-HAEA exhibited similar affinity for both human CB_1 and CB_2 receptors, and significantly (~70–90-fold and ~40–60-fold) lower affinity than the parent compound anandamide, as shown in Table 1.

DISCUSSION

The first aim of this study was to investigate whether or not anandamide, an endocannabinoid and endovanilloid mediator, can be transformed by the *Candida* cognate fungus *D. uninucleata* into its 3-hydroxy derivative. Additionally, in order to assist with the identification of putative 3-HAEA from the conversion experiments and eventually obtain it in amounts sufficient to profile its activity at cannabinoid and TRPV1 receptors, we have synthesized here for the first time 3(*R*)- and 3(*S*)-HAEA. We have shown that these synthetic compounds are chromatographically and mass-spectrometrically indistinguishable from a metabolite obtained after incubation of *D. uninucleata* with anandamide, and that, compared with the latter compound, they exhibit dramatically reduced binding activity at both cannabinoid receptors types, while retaining activity at TRPV1 receptors, as shown by their capability to increase intracellular Ca^{2+} and to induce cation-mediated currents in HEK-293 cells overexpressing human recombinant TRPV1 channels.

Anandamide affinity and functional potency at TRPV1 receptors are about one order of magnitude lower than those at CB_1 receptors (30–32). Therefore, endogenous anandamide can be predicted to act predominantly as an endocannabinoid and, by activating CB_1 and CB_2 receptors, to inhibit the pronociceptive and proinflammatory actions of TRPV1 agonists (33, 34). However, anandamide was shown to activate TRPV1 receptors when CB_1 receptors are blocked and/or when TRPV1 channels are sensitized by stimuli, like those occurring during inflammatory reactions (17, 18, 35–39). TRPV1 sensitization likely occurs during candidiasis, because increased expression of vulvar TRPV1 receptors is observed during vulvodynia, a condition similar to that caused by candidiasis (14), and clotrimazole, a widely used antimycotic agent, was suggested to owe its inflamma-

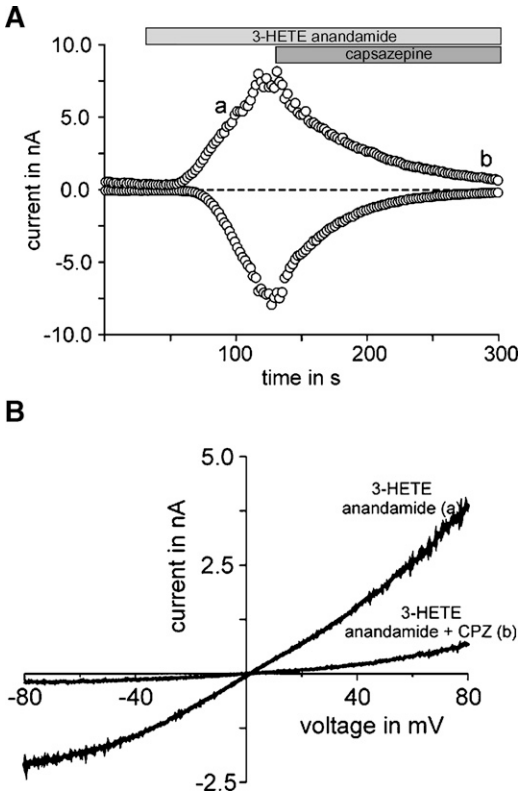

Fig. 5. TRPV1 can be activated by 3(R)-hydroxy-anandamide in whole-cell patch clamp recordings. A: Representative example of a whole cell patch clamp recording of HEK-293 cells overexpressing the human recombinant TRPV1 in response to 3(*R*)-hydroxy-anandamide (n = 8), here denoted as "3-HETE-anandamide." Data are gathered from voltage-ramps and depict the current at +80 mV and −80 mV. The zero current level is indicated by the dashed line. Lowercase 'a' refers to traces obtained in the absence of capsazepine (CPZ); lowercase 'b' refers to traces obtained in the presences of CPZ. B: 500 ms voltage ramp from −80 mV to +80 mV applied at the time points indicated as in A. 3(*R*)-hydroxy-anandamide and the TRPV1 antagonist, capsazepine were applied at concentrations of 20 μM and 10 μM, respectively.

tory and algogenic side effects to its capability to activate TRPV1 receptors (40). On the other hand, several peripheral inflammatory conditions causing pain and/or itch are known to be accompanied by elevated levels of anandamide as an adaptive reaction to counteract these symptoms, as suggested by the observation that compounds that prolong the life span of anandamide by inhibiting its inactivation exert anti-inflammatory effects (15, 16, 41–47). Thus, it seems reasonable to hypothesize that, during candidiasis-induced inflammation, on the one hand TRPV1 is sensitized, and, on the other hand, anandamide is produced by host or neighboring cells. Thus, *Candida* species might partly transform endogenously produced anandamide into 3-HAEA, as observed here for *D. uninucleata*, thus leading to the formation of a predominantly antihyperalgesic and anti-inflammatory mediator into a "pure" TRPV1 agonist. This mechanism might contribute to some of the typical symptoms of candidiasis.

Clearly, further experiments that are beyond the aims of the present study are needed in order to corroborate or rule out this hypothesis. First, it will be necessary to assess if the conversion of anandamide into 3-HAEA does occur also during candidiasis, and, if so, to what extent. The production of 3-hydroxyeicosanoids like 3-hydroxyPGE_2 upon infection of HeLa cells with *C. albicans* supports the hypothesis that also 3-HAEA might be formed during infection with this pathogenic fungus (23). On the other hand, still enough endogenous anandamide to activate CB_1 and CB_2 receptors might remain even if this conversion were to occur in vivo, and this would counteract the effects of 3-HAEA. A second issue for future studies should be the assessment of the relative regulation of TRPV1 and cannabinoid receptors during candidiasis. Furthermore, the activity of 3-HAEA should also be investigated in "native" cells that constitutively express TRPV1 receptors, since a higher potency has been reported, at least for anandamide, at activating these channels when they are overexpressed in cells (30–32). Finally, the configuration of 3-HAEA produced from *D. uninucleata* needs to be investigated to clarify if this compound is produced through the same pathway (β-oxidation) as 3(*R*)-HETE, as it might seem unlikely given the fact that anandamide is not capable of making the ester with CoA, which is necessary for entering this catabolic route. The alternative possibility that 3-HAEA is produced by cytochrome p450/oxigenase-catalyzed 3-hydroxylation of anandamide would be, instead, suggested by the fact that this latter compound is recognized as substrate by several enzymes of the AA cascade (24). At any rate, we have shown here that the configuration of 3-HAEA has little biological relevance in terms of activation of either TRPV1 or cannabinoid receptors. It would be also important to assess if the other major endocannabinoid, 2-arachidonoylglycerol, which has little activity at TRPV1 receptors (30–32), and is more abundant than anandamide in tissues, is converted by 3-(*R*)-HETE-producing fungi.

In conclusion, we have provided evidence that a 3-HETE-producing fungus can act in vitro upon the anandamide potentially released by host or neighboring cells during candidiasis, thus catalyzing its transformation into a compound that is no longer capable to activate cannabinoid receptors but retains agonist activity at the TRPV1 channel. Our study might suggest that compounds capable to prolong the lifespan of anandamide by inhibiting its inactivation, and that have proved useful in several animal models of pain, inflammation, and itch (15, 16, 41–48), might not be necessarily suitable for the symptomatic treatment of candidiasis, as they might also promote the formation of 3-HAEA, a likely algogenic compound. Furthermore, our data provide an unusual example of the typical capability of pathogenic microorganisms to control, or even exploit, innate defense mechanisms to facilitate infection (49, 50).

The authors thank Mr. Marco Allarà, Endocannabinoid Research Group, CNR, Italy for his technical assistance in binding assays.

REFERENCES

1. Maksymiuk, A. W., S. Thongprasert, R. Hopfer, M. Luna, V. Fainstein, and G. P. Bodey. 1984. Systemic candidiasis in cancer patients. *Am. J. Med.* **77:** 20–27.
2. Meunier, F. 1987. Prevention of mycoses in immunocompromised patients. *Rev. Infect. Dis.* **9:** 408–416.
3. Antrum, J. 1996. Meeting the challenge of systemic fungal infections in cancer: nursing implications. *Eur. J. Haematol. Suppl.* **57:** 7–11.
4. Lew, M. A. 1989. Diagnosis of systemic Candida infections. *Annu. Rev. Med.* **40:** 87–97.
5. Bow, E. J. 1998. Invasive fungal infections in patients receiving intensive cytotoxic therapy for cancer. *Br. J. Haematol.* **101(Suppl. 1):** 1–4.
6. De Pauw, B. E., and J. F. Meis. 1998. Progress in fighting systemic fungal infections in haematological neoplasia. *Support. Care Cancer.* **6:** 31–38.
7. Sobel, J. D. 1990. Vaginal infections in adult women. *Med. Clin. North Am.* **74:** 1573–1601.
8. Odds, F. C. 1988. Genital candidosis. In Candida and candidosis; a review and bibliography. F. C. Odds, editor 2nd ed., Baillière Tindall, London 124–135
9. Lindler, J. G., F. H. Plantema, and J. A. Hoogkamp-Korstange. 1978. Quantative studies of the vaginal flora of healthy women and of obstetric and gynaecologic patients. *J. Med. Microbiol.* **11:** 233–241.
10. Caterina, M. J., M. A. Schumacher, M. Tominaga, T. A. Rosen, J. D. Levine, and D. Julius. 1997. The capsaicin receptor: a heat-activated ion channel in the pain pathway. *Nature.* **389:** 816–824.
11. Szallasi, A., D. N. Cortright, C. A. Blum, and S. R. Eid. 2007. The vanilloid receptor TRPV1: 10 years from channel cloning to antagonist proof-of-concept. *Nat. Rev. Drug Discov.* **6:** 357–372.
12. Starowicz, K., S. Nigam, and V. Di Marzo. 2007. Biochemistry and pharmacology of endovanilloids. *Pharmacol. Ther.* **114:** 13–33.
13. Starowicz, K., L. Cristino, and V. Di Marzo. 2008. TRPV1 receptors in the central nervous system: potential for previously unforeseen therapeutic applications. *Curr. Pharm. Des.* **14:** 42–54.
14. Tympanidis, P., M. A. Casula, Y. Yiangou, G. Terenghi, P. Dowd, and P. Anand. 2004. Increased vanilloid receptor VR1 innervation in vulvodynia. *Eur. J. Pain.* **8:** 129–133.
15. Jayamanne, A., R. Greenwood, V. A. Mitchell, S. Aslan, D. Piomelli, and C. W. Vaughan. 2006. Actions of the FAAH inhibitor URB597 in neuropathic and inflammatory chronic pain models. *Br. J. Pharmacol.* **147:** 281–288.
16. Mitchell, V. A., R. Greenwood, A. Jayamanne, and C. W. Vaughan. 2007. Actions of the endocannabinoid transport inhibitor AM404 in neuropathic and inflammatory pain models. *Clin. Exp. Pharmacol. Physiol.* **34:** 1186–1190.
17. De Petrocellis, L., S. Harrison, T. Bisogno, M. Tognetto, I. Brandi, G. D. Smith, C. Creminon, J. B. Davis, P. Geppetti, and V. Di Marzo. 2001. The vanilloid receptor (VR1)-mediated effects of anandamide are potently enhanced by the cAMP-dependent protein kinase. *J. Neurochem.* **77:** 1660–1663.
18. Ahluwalia, J., L. Urban, S. Bevan, and I. Nagy. 2003. Anandamide

regulates neuropeptide release from capsaicin-sensitive primary sensory neurons by activating both the cannabinoid 1 receptor and the vanilloid receptor 1 in vitro. *Eur. J. Neurosci.* **17:** 2611–2618.
19. van Dyk, M. S., J. L. Kock, D. J. Coetzee, O. P. Augustyn, and S. Nigam. 1991. Isolation of a novel arachidonic acid metabolite 3-hydroxy-5,8,11,14-eicosatetraenoic acid (3-HETE) from the yeast Dipodascopsis uninucleata UOFs-Y128. *FEBS Lett.* **283:** 195–198.
20. Deva, R., R. Ciccoli, T. Schewe, J. L. Kock, and S. Nigam. 2000. Arachidonic acid stimulates cell growth and forms a novel oxygenated metabolite in Candida albicans. *Biochim. Biophys. Acta.* **1486:** 299–311.
21. Deva, R., R. Ciccoli, L. Kock, and S. Nigam. 2001. Involvement of aspirin-sensitive oxylipins in vulvovaginal candidiasis. *FEMS Microbiol. Lett.* **198:** 37–43.
22. Deva, R., P. Shankaranarayanan, R. Ciccoli, and S. Nigam. 2003. Candida albicans induces selectively transcriptional activation of cyclooxygenase-2 in HeLa cells: pivotal roles of Toll-like receptors, p38 mitogen-activated protein kinase, and NF-kappa B. *J. Immunol.* **171:** 3047–3055.
23. Ciccoli, R., S. Sahi, S. Singh, H. Prakash, M. P. Zafiriou, G. Ishdorj, J. L. Kock, and S. Nigam. 2005. Oxygenation by COX-2 (cyclooxygenase-2) of 3-HETE (3-hydroxyeicosatetraenoic acid), a fungal mimetic of arachidonic acid, produces a cascade of novel bioactive 3-hydroxyeicosanoids. *Biochem. J.* **390:** 737–747.
24. Marnett, L. J. 2002. Recent developments in cyclooxygenase inhibition. *Prostaglandins Other Lipid Mediat.* **68–69:** 153–164.
25. Bhatt, R. K., J. R. Falck, and S. Nigam. 1998. Enantiospecific total synthesis of a novel arachidonic acid metabolite, 3-hydroxyeicosatetraenoic acid. *Tetrahedron Lett.* **39:** 249–252.
26. Groza, N., I. V. Ivanov, S. G. Romanov, G. I. Myagkova, and S. Nigam. 2002. A novel synthesis of 3(R)-HETE, 3(R)-HTDE and enzymatic synthesis of 3(R), 15(S)- diHETE. *Tetrahedron.* **58:** 9859–9863.
27. Fried, J., J. C. Sih, C. H. Lin, and P. Dalven. 1972. Regiospecific epoxide opening with acetylenic alanes. Improved total synthesis of E and F prostaglandins. *J. Am. Chem. Soc.* **94:** 4343–4345.
28. Ivanov, I. V., S. G. Romanov, N. V. Groza, S. Nigam, H. Kuhn, and G. I. Myagkova. 2002. A simple method for the preparation of (5Z,8Z,11Z,14Z)-16-Hydroxyeicosa-5,8,11,14-tetraenoic acid enantiomers and the corresponding 14,15-Dehydro analogues: role of the 16-Hydroxy group for the lipoxygenase reaction. *Bioorg. Med. Chem.* **10:** 2335–2343.
29. Appendino, G., A. Minassi, S. Schiano Moriello, L. De Petrocellis, and V. Di Marzo. 2002. N-Acylvanillamides: development of an expeditious synthesis and discovery of new acyl templates for powerful activation of the vanilloid receptor. *J. Med. Chem.* **45:** 3739–3745.
30. Zygmunt, P. M., J. Petersson, D. A. Andersson, H. Chuang, M. Sørgård, V. Di Marzo, D. Julius, and E. D. Högestätt. 1999. Vanilloid receptors on sensory nerves mediate the vasodilator action of Anandamide. *Nature.* **400:** 452–457.
31. Smart, D., M. J. Gunthorpe, J. C. Jerman, S. Nasir, J. Gray, A. I. Muir, J. K. Chambers, A. D. Randall, and J. B. Davis. 2000. The endogenous lipid anandamide is a full agonist at the human vanilloid receptor (hVR1). *Br. J. Pharmacol.* **129:** 227–230.
32. De Petrocellis, L., T. Bisogno, J. B. Davis, R. G. Pertwee, and V. Di Marzo. 2000. Overlap between the ligand recognition properties of the anandamide transporter and the VR1 vanilloid receptor: inhibitors of anandamide uptake with negligible capsaicin-like activity. *FEBS Lett.* **483:** 52–56.
33. Richardson, J. D., S. Kilo, and K. M. Hargreaves. 1998. Cannabinoids reduce hyperalgesia and inflammation via interaction with peripheral CB1 receptors. *Pain.* **75:** 111–119.
34. Hermann, H., L. De Petrocellis, T. Bisogno, A. Schiano Moriello, B. Lutz, and V. Di Marzo. 2003. Dual effect of cannabinoid CB1 receptor stimulation on a vanilloid VR1 receptor-mediated response. *Cell. Mol. Life Sci.* **60:** 607–616.
35. Morisset, V., J. Ahluwalia, I. Nagy, and L. Urban. 2001. Possible mechanisms of cannabinoid-induced antinociception in the spinal cord. *Eur. J. Pharmacol.* **429:** 93–100.
36. De Petrocellis, L., T. Bisogno, M. Maccarrone, J. B. Davis, A. Finazzi-Agrò, and V. Di Marzo. 2001. The activity of anandamide at vanilloid VR1 receptors requires facilitated transport across the cell membrane and is limited by intracellular metabolism. *J. Biol. Chem.* **276:** 12856–12863.
37. Dinis, P., A. Charrua, A. Avelino, M. Yaqoob, S. Bevan, I. Nagy, and F. Cruz. 2004. Anandamide-evoked activation of vanilloid receptor 1 contributes to the development of bladder hyperreflexia and nociceptive transmission to spinal dorsal horn neurons in cystitis. *J. Neurosci.* **24:** 11253–11263.
38. Singh Tahim, A., P. Sántha, and I. Nagy. 2005. Inflammatory mediators convert anandamide into a potent activator of the vanilloid type 1 transient receptor potential receptor in nociceptive primary sensory neurons. *Neuroscience.* **136:** 539–548.
39. Evans, R. M., R. H. Scott, and R. A. Ross. 2007. Chronic exposure of sensory neurones to increased levels of nerve growth factor modulates CB1/TRPV1 receptor crosstalk. *Br. J. Pharmacol.* **152:** 404–413.
40. Meseguer, V., Y. Karashima, K. Talavera, D. D'Hoedt, T. Donovan-Rodríguez, F. Viana, B. Nilius, and T. Voets. 2008. Transient receptor potential channels in sensory neurons are targets of the antimycotic agent clotrimazole. *J. Neurosci.* **28:** 576–586.
41. Lichtman, A. H., D. Leung, C. C. Shelton, A. Saghatelian, C. Hardouin, D. L. Boger, and B. F. Cravatt. 2004. Reversible inhibitors of fatty acid amide hydrolase that promote analgesia: evidence for an unprecedented combination of potency and selectivity. *J. Pharmacol. Exp. Ther.* **311:** 441–448.
42. Holt, S., F. Comelli, B. Costa, and C. J. Fowler. 2005. Inhibitors of fatty acid amide hydrolase reduce carrageenan-induced hind paw inflammation in pentobarbital-treated mice: comparison with indomethacin and possible involvement of cannabinoid receptors. *Br. J. Pharmacol.* **146:** 467–476.
43. La Rana, G., R. Russo, P. Campolongo, M. Bortolato, R. A. Manieri, V. Cuomo, A. Iacono, G. M. Raso, R. Meli, D. Pomelli, et al. 2006. Modulation of neuropathic and inflammatory pain by the endocannabinoid transport inhibitor AM404. [N-(4-hydroxyphenyl)-eicosa-5,8,11,14-tetraenamide] *J. Pharmacol. Exp. Ther.* **317:** 1365–1371.
44. Chang, L., L. Luo, J. A. Palmer, S. Sutton, S. J. Wilson, A. J. Barbier, J. G. Breitenbucher, S. R. Chaplan, and M. Webb. 2006. Inhibition of fatty acid amide hydrolase produces analgesia by multiple mechanisms. *Br. J. Pharmacol.* **148:** 102–113.
45. D'Argenio, G., M. Valenti, G. Scaglione, V. Cosenza, I. Sorrentini, and V. Di Marzo. 2006. Up-regulation of anandamide levels as an endogenous mechanism and a pharmacological strategy to limit colon inflammation. *FASEB J.* **20:** 568–570.
46. Karsak, M., E. Gaffal, R. Date, L. Wang-Eckhardt, J. Rehnelt, S. Petrosino, K. Starowicz, R. Steuder, E. Schlicker, B. Cravatt, et al. 2007. Attenuation of allergic contact dermatitis through the endocannabinoid system. *Science.* **316:** 1494–1497.
47. Michalski, C. W., T. Laukert, D. Sauliunaite, P. Pacher, F. Bergmann, N. Agarwal, Y. Su, T. Giese, N. A. Giese, S. Bátkai, et al. 2007. Cannabinoids ameliorate pain and reduce disease pathology in cerulein-induced acute pancreatitis. *Gastroenterology.* **132:** 1968–1978.
48. Di Marzo, V., T. Bisogno, and L. De Petrocellis. 2007. Endocannabinoids and related compounds: walking back and forth between plant natural products and animal physiology. *Chem. Biol.* **14:** 741–756.
49. Donnenberg, M. S., J. B. Kaper, and B. B. Finlay. 1997. Interactions between enteropathogenic Escherichia coli and host epithelial cells. *Trends Microbiol.* **5:** 109–114.
50. TranVan Nhieu, G., C. Clair, G. Grompone, and P. Sansonetti. 2004. Calcium signalling during cell interactions with bacterial pathogens. *Biol. Cell.* **96:** 93–101.